

## ARTICLE TYPE

# Visualization Modality for Augmented Reality Guidance of in-depth Tumour Enucleation Procedures

Nadia Cattari<sup>1,2</sup> | Fabrizio Cutolo<sup>1,2</sup> | Luciana La Placa<sup>1</sup> | Vincenzo Ferrari<sup>1,2</sup><sup>1</sup>Department of Information Engineering, University of Pisa, Italy<sup>2</sup>EndoCAS Centre, University of Pisa, Italy**Correspondence**

Corresponding author Nadia Cattari.

Email: nadia.cattari@unipi.it

**Present address**

Cisanello Hospital, Building 102, Via Paradisa 2, 56124, Pisa, Italy

**Abstract**

Recent research studies reported that the employment of wearable Augmented Reality (AR) systems such as Head-Mounted Displays (HMDs) for the in-situ visualization of ultrasound (US) images can improve the outcomes of US-guided biopsies through reduced procedure completion times and improved accuracy. In this work, we continue in the direction of recent developments and we present the first AR system for guiding an in-depth tumour enucleation procedure under US guidance. The system features an innovative visualization modality with cutting trajectories that "sink" into the tissue according to the depth reached by the electric scalpel, tracked in real-time, and a virtual-to-virtual alignment between the scalpel's tip and the trajectory. The system has high accuracy in estimating the scalpel's tip position (mean depth error of 0.4 mm and mean radial error of 1.34 mm). Furthermore, we demonstrated with a preliminary user study that our system allowed to successfully guide an in-depth tumour enucleation procedure (i.e., preserving the safety margin around the lesion).

**KEY WORDS**

Augmented reality, in-depth guidance, tumour enucleation, visualization modality.

## 1 | INTRODUCTION

In recent years, the increasing availability of Augmented Reality (AR) systems easily customizable and at ever more affordable prices, has given a major boost to research in the healthcare sector for the implementation of this technology in the medical and surgical field<sup>1</sup>. AR systems based on wearable technologies such as Head-Mounted Displays (HMDs) enable the augmentation of the real scene with virtual information useful for the surgical act (i.e., patient's vital parameters, virtual 3D model of anatomical details, insertion and/or cutting trajectories, etc) displayed directly along the operator's line of sight, preserving the egocentric point of view and thus reducing the visual motor field disparity inherent in image-guided procedures<sup>2,3</sup>.

The employment of wearable AR systems for a direct overlay of Ultrasound (US) images onto the according anatomy has been envisioned and studied since the mid-1990s. The visualization of the target in its current physical position through AR can in fact improve the outcome on the US-guided intervention both in terms of completion time and improved accuracy. In 1996, Fuchs et al.<sup>4</sup> first proposed the implementation of a prototype AR system to aid the clinician performing US-guided needle biopsies. They used a wearable AR visor to guide the biopsy task on both phantom experiments and human subjects' experiments. The system merged US data with images of the surgical field acquired by the cameras mounted on the HMD and provided the merged images on the HMD displays. By means of AR, the authors rendered a "synthetic opening – a virtual "pit" – embedded within the patient"<sup>4</sup>. The US slices acquired with the 2D probe are displayed within this opening, thus visualised in-situ in a 1:1 ratio. Despite some limitations mainly due to the backwardness of the system implied (e.g., cumbersome equipment, inadequate tracking technology, etc.) the clinician was able to use the AR guidance to insert the needle in a synthetic tumour within a breast phantom and examine a human patient in preparation for a cyst aspiration.

Within the same research group, in 2002 Rosenthal et al.<sup>5</sup> conducted a quantitative study of 50 biopsies (25 performed with traditional approach and 25 with the aid of an AR system) to compare the accuracy of standard US-guided needle biopsy to

**Abbreviations:** AR, Augmented Reality, FOV, field of view, HMDs, Head-Mounted Displays, OST, Optical See-Through, VST, Video See-Through, US, Ultrasound.

biopsies performed using a 3D AR guiding system. Medical data were acquired with a 2D US probe whilst the AR HMD employed was lighter and more ergonomic version of the visor used in the previous work. Experimental results showed that the mean error in terms of deviation from the desired target was statistically significantly smaller in the HMD method than in the standard one, which suggests that AR systems can provide higher accuracy over traditional biopsy guidance methods.

The same year, a similar work was proposed by<sup>6</sup>, involving the integration of an AR HMD and a US imaging system. In this case, the 2D US slice was displayed in-situ within a "virtual hole" registered over the phantom. The purpose of this work was mainly to present the developed system, its feature, and specifications, and to explain the calibration methods implemented. No quantitative or qualitative studies on the accuracy of the system were conducted. However, it represented a further step toward the successful integration of these two technologies and the active research interest in this field.

In recent years, the development of AR systems, which has led to improved readiness and maturity of this technology, and the clinical thrust toward minimally invasive approaches, have boosted research in this area. In 2016 Kanithi et al.<sup>7</sup> presented a further work on the US-AR integration. In their work, assistance with needle insertion was provided to the clinician through an AR HMD. Besides being able to visualise the 2D US slice in-situ correctly registered over the phantom, the clinician could also see in AR the needle tip, the needle insertion trajectory, and the out-of-plane alignment error. Even though this work lacked a user study with a quantitative evaluation of the error committed by the clinician and a qualitative evaluation of the system usability, the assessments carried out in terms of the accuracy provided by the system were more than encouraging.

In 2020, R ger et al.<sup>8</sup> conducted a quantitative user study to compare the user's performances between the traditional and the AR methods during a 2D US-guided needle insertion. The AR methods entailed the visualization of the US image in-situ, spatially correctly aligned under the US transducer, by means of a first-generation Microsoft HoloLens. The results showed that the participants were significantly more accurate, in terms of needle placement error, when using the AR HMD, with a reduction of the error of a third. The same year, Farshad-Amacker et al.<sup>9</sup> published another comparative study based on 200 biopsies (100 performed with the AR aid and 100 without), to determine whether the use of AR had an influence on the task execution times and the number of needle passes required to reach the target. Here again, the authors employed Microsoft HoloLens as AR HMD to show the 2D US slice as anchored to the probe and registered over the phantom. The experimental results showed that the AR in-situ US visualization saved time and needle passes through all operators.

In 2021, an alternative method for US guidance of biopsies using AR was proposed<sup>10</sup>. Rather than displaying the 2D slice, a 3D virtual model of the target lesion, derived from a 3D US scan, was presented to the user via the AR HMD. To guide the biopsy needle to the target, the operator had to align the needle along the correct trajectory by means of two virtual viewfinders added to the AR scene. With this guidance modality, 80% of the users were able to biopsy a 5 mm diameter target lesion. Further progress in this direction was achieved by<sup>11</sup> in 2023, who developed the first application allowing in-situ visualization of real-time volumetric US acquisition for vascular puncture guidance. The authors compared the combination of 3D US with AR versus 2D US with AR to determine whether the volumetric visualization could indeed offer additional benefits in procedure outcomes. Their results showed a significant improvement in task execution time (a 28.4% decrease in execution time with the 3D US AR compared to the 2D US AR), along with an improvement in vascular puncture success rate (2D US AR - 50% compared to 3D US AR - 72%) although not statistically significant.

However, the previously mentioned works all concern needle insertion interventions. To the best of the authors' knowledge, no system has yet been presented in the literature that aims to guide more challenging in-depth interventions, such as tumour enucleation. In this procedure, the surgeon excises the lesion cutting around it while leaving an appropriate safety margin, to avoid the risk of incising the malignant tissue<sup>12</sup>. In addition to visualizing the tumour in its physical position, to guide the procedure it is thus necessary to keep track in real-time of the instrument's tip. However, the visualisation modality already proposed in a previous study<sup>13</sup>, which featured the cutting line "lying" on the surface to be incised, cannot be used for the enucleation procedure. To correctly perform an in-depth incision following a trajectory projected solely on the surface, the operator needs to steadily maintain his/her point of view coaxial with the insertion axis. If this requirement is not met, an error related to the parallax between the ideal and the real point of view is committed<sup>14</sup>, as shown in Figure 1. Moreover, as the surgical tool goes deeper into the tissue, it becomes difficult to identify the position of its tip due to occlusions (e.g., the blood prevents the tip from being correctly visualized).

In this study, we propose an innovative visualization modality for guiding in-depth tumour enucleation. In our system, the virtual trajectory used to guide the incision is shown at progressively increasing depths depending on the scalpel penetration into the tissue. By varying the trajectory according to the scalpel depth, determined in real-time through the instrument's tracking, we are therefore able to provide the correct guidance regardless of the operator's point of view. Moreover, to overcome the occlusions

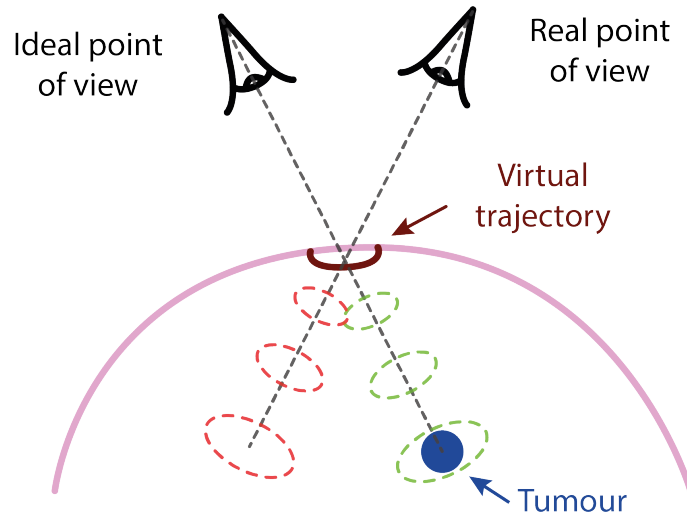


**FIGURE 1** When the point of view of the operator is aligned and coaxial with the ideal entry axis, cutting in-depth along this trajectory would lead to the lesion. If the operator changes his/her point of view, a parallax-related error (directly proportional to the entity of the offset) is committed.

that prevent the visualization of the real tip once is inserted into the tissue, we implemented a virtual-to-virtual alignment guiding technique: the virtual sphere, associated with the instrument tip, has to be moved within virtual track-like cutting guides.

## 2 | AR SYSTEM DESCRIPTION

The system used in the experiments is the VOSTARS wearable AR system, which consists of two major components: the hybrid Optical/Video See-Through HMD and the computational and navigation platform. The HMD is a re-engineered version of a commercial binocular Optical See-Through (OST) visor (ARS.30 by Trivisio<sup>15</sup>), customized to make it hybrid. The transition between the two AR visualization modalities, OST and Video See-Through (VST), is provided through a pair of liquid-crystal (LC) optical shutters, whose transparency can be electronically dimmed according to the voltage supplied at their ends<sup>16</sup>. The LC panels are placed in front of the two optical combiners of the ARS.30, whose microdisplay features a  $1280 \times 1024$  resolution at 60 Hz refresh rate and  $30^\circ$  diagonal field of view (FOV), which corresponds to  $\approx 1.11$  arcmin/pixel angular resolution, close to the human visual acuity<sup>17</sup>. The VST paradigm is provided through a pair of world-facing RGB cameras, the LI-OV4689 by Leopard Imaging, incorporated within the 3D plastic shell that holds the ARS.30 and the two LC panels. The two cameras are equipped with  $1/3''$  OmniVision CMOS 4M pixels sensor and M12 lens with 6 mm focal length lens and are set with a configuration of  $2 \times 1280 \times 720@60$  fps. To ensure a quasi-orthostereoscopic perception of the real scene in VST modality, the cameras have an anthropometric interaxial distance ( $\approx 6.3$  cm) and a fixed convergence angle of  $3.4^\circ$ . This solution provides sufficient stereo overlap at about 40 cm (i.e., the average working distance for manual tasks) and mitigates the horizontal disparity due to camera-to-eye parallax. The stereo cameras are also employed for the inside-out optical tracking featured by the AR platform, which is based on OpenCV API 3.4.1 and performs the stereo localization of a triple of monochrome spherical markers. The tracking information is exploited by the software to augment the scene, both in OST and VST: the virtual objects, constrained to the tracked triple, are rendered onto the displays registered on the reality ensuring locational realism<sup>18</sup>. The AR navigation platform supports the in-situ visualization of medical data using VTK libraries, an open-source library for 3D computer graphics, modeling, and volume rendering. The software framework is based on Computer Unified Device Architecture (CUDA), a multithread architecture that allows significant computational efficiency and ensures high flexibility both in terms of renderable contents and tracking capability. In particular, the multi-thread architecture enables an average frame rate of  $\approx 30$  fps to be obtained for each eye.

For the purpose of this work, the AR system was used in VST modality combined with the medical data provided by a 3D US acquisition system (the Philips iU22 coupled with the Philips VL 13-5 probe). To ensure the proper locational realism, thus in order for the virtual content extrapolated from the volumetric US acquisition to be correctly spatially registered over the real

scene, the relative pose between the AR visor and the US acquisition needed to be known at all time. This required a dedicated calibration procedure, which is thoroughly described in<sup>10</sup>.

### 3 | SYSTEM OPTIMIZATION

#### 3.1 | Electric scalpel sensorization and calibration

In consultation with the surgeons, we employed an electric scalpel in place of a regular one, as they claimed it to be the most commonly used surgical tool in enucleation procedures. In particular, a needle-tipped electrode was chosen, since its symmetry allows easy identification of the tip. As mentioned in Section 2, the AR platform exploits the stereo localization of a triple of spherical markers to determine the position and orientation of an object (e.g., the US probe) in the real scene. Thus, to be tracked in real-time within the AR system, the electric scalpel required a similar sensorization. An optical frame formed by three spherical markers was designed with Creo Parametrics 6.0, 3D printed and uniquely anchored to the scalpel. As shown in Figure 2, the markers were coloured in fluorescent red to improve visibility and strengthen the RGB tracking.

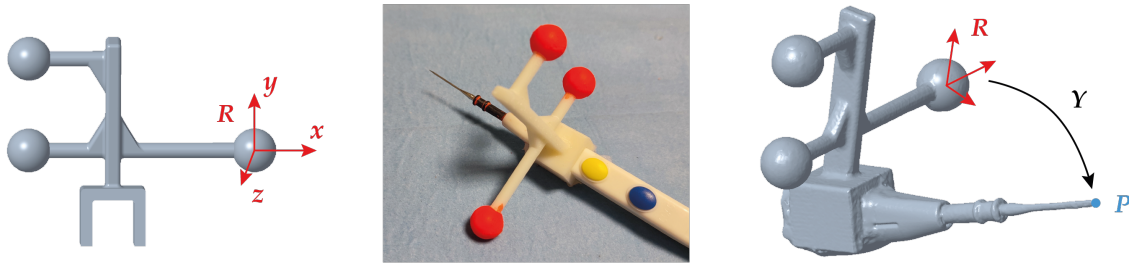


**FIGURE 2** Optical frame designed for the sensorization of the scalpel. From left to right: CAD perspective view; the electric scalpel sensorized, the spherical markers were dyed in red to improve the strength of the tracking; 3D scan of the scalpel with the  $Y$  matrix identifying the position of the scalpel tip with respect to the reference system of the optical frame.

To spatially register the virtual sphere associated with the tip of the scalpel over the actual scalpel tip ( $P$ ), the rigid relation between the tip and the reference system of the optical frame ( $R$ ) was required ( $Y$  transformation in Figure 2). This was obtained through a calibration procedure performed with the EinScan-SE 3D Scanner by Shining 3D, who declares a single shot accuracy of  $\leq 0.1mm$ . The STL file derived from the 3D scan was imported on Creo Parametrics 6.0 where the rigid relation between  $P$  and  $T$  (transformation  $Y$  in Figure 2) could be derived.

#### 3.2 | Post-calibration accuracy assessment

An experiment was carried out to assess the soundness of the calibration and the accuracy that the AR system has in providing the distance between the electric scalpel tip and a potential target (i.e., the lesion to be removed). The task devised was a targeting task, which consisted in reaching known points in space with the scalpel tip and evaluating the Euclidian distance between the position of the tip provided by the AR system as output, and the actual coordinates of the known points, both related to the AR system's reference system, associated with the HMD. The known points belonged to a phantom designed and 3D printed for the purpose. It featured the usual three spherical markers and a viewfinder with two concentric circles of known dimensions (15 and 30 mm in diameter). The triple of markers was coloured in fluorescent green, and was designed with a geometry slightly different compared to the scalpel optical frame in order to ease the distinction of the two objects for the tracking algorithm. The local reference system  $M$  of the viewfinder has its origin at the centre of the viewfinder,  $y$ -axis and  $z$ -axis belonging to the viewfinder plane and  $x$ -axis orthogonal to the plane, as depicted in Figure 3. For the test, the visor was anchored on a mounting arm and positioned so as to frame the phantom within the cameras FOV. The scalpel tip was placed at 21 known points: 12 on the outer circles, 8 on the inner circle, and 1 at the centre of the viewfinder.

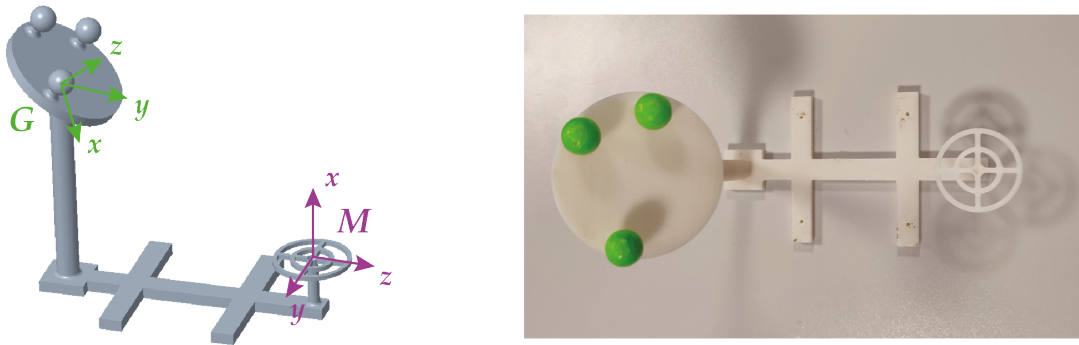


**FIGURE 3** Sensorized 3D printed viewfinder designed for the accuracy assessment experiment. From left to right: the CAD perspective view with the two reference system  $G$  and  $M$  indicated; the viewfinder 3D printed and dyed.

### 3.3 | Accuracy assessment results

For each of the 21 points, the Euclidean distance between the actual and the estimated position of the scalpel tip was calculated. Accuracy was then assessed in terms of radial and depth error. Table 1 reports the results of the error analysis.

**TABLE 1** Radial and depth errors in mm.

Errors	Mean	Median	Max
Radial	1.34	1.5	2.93
Depth	0.4	0.37	1.08

The results of the experiment are quite positive. They show that the AR system can provide the position of the instrument tip with high accuracy, both in terms of depth relative to the target to be reached (i.e., the viewfinder, in this case) and in radial terms relative to it. In particular, even the maximum error registered stays within the range of alternative mechatronic and robotic-assisted systems proposed in the literature, with reported system errors in the range of  $1 \sim 3$  mm<sup>19,20</sup>.

## 4 | AR GUIDANCE OF AN ENUCLEATION PROCEDURE

### 4.1 | Design of the innovative visualisation modality

In consultation with clinicians who are experts in the tumour enucleation procedure, we devised a new visualisation modality to effectively guide the resection of an in-depth lesion. It allows the operator to visualize the correct cutting trajectory according to the depth reached by the electric scalpel. Moreover, a concern arose by the clinicians was the impossibility to perform a real-to-virtual alignment once the scalpel is deep into the tissue, due to the difficulty of identifying the scalpel tip once it has penetrated. To address this issue, we decided to implement a virtual-to-virtual alignment guiding technique. The cutting trajectories consist of two concentric circumferences centred on the lesion, similar to a track. The operator's objective is therefore to perform the cut while keeping the virtual sphere (2 mm in diameter) associated with the scalpel tip within the track.

The diameters of the two circumferences forming the track were chosen according to the errors obtained in the accuracy test previously described, i.e., the maximum radial error of  $\approx 3$  mm. Bearing this in mind, for a lesion of 10 mm in diameter, the ideal cutting trajectory has a radius of 15 mm (5 mm the lesion radius + 10 mm the safety margin), and the two circumferences have a radius  $\pm 3$  mm the ideal cutting trajectory. The ideal trajectory within the track has thus a radius of 18 mm, whilst the spacing between the two circumferences forming the track is 6 mm. The enucleated volume will therefore be a cylinder,  $\approx 36$  mm in diameter (depending on the operator's precision in following the cutting trajectories) and varying in height depending on

the depth of the lesion from the entry surface. The distance between the entry point on the surface and the lesion, which is the ideal axis of the enucleation cylinder, was divided into planes orthogonal to the axis and equidistant from each other. On each of these planes, one of the cutting trajectories above described was created, and could thus be visualised by the operator during the task. repeated at several planes orthogonal to the ideal insertion axis joining the entry point on the surface and the lesion

Chromatic information was also added to the augmented scene to give the operator additional visual feedback about the position of the scalpel tip<sup>21</sup>. As depth information, in addition to numerically displaying the distance between the scalpel tip and the lesion at the top left corner of the display, the trajectories were coloured in different shades as one goes deeper, from yellow to dark red. As radial information, a semaphore was added at the bottom left corner: it turns green if the scalpel tip is within the track, red if it goes inside the inner circumference, and yellow if it lies outside the outer circumference.

## 4.2 | Experimental setup and protocol

Four non-clinical users were asked to test the system by wearing the AR HMD and performing a simulated enucleation task. The procedures were performed on customized phantoms made with agar and comprising a polyvinyl chloride (PVC) lesion 10 mm in diameter at a known depth. For the acquisition of the lesion, a 3D US probe was used, anchored to a mounting arm and properly sensorized with a triple of spherical markers so as to be tracked in real-time by the AR system. The lesion was at 3.2 cm from the entry surface, thus the maximum depth of cut was at 4.7 cm (3.2 cm the centre of the lesion + 0.5 cm the lesion radius + 1 cm the safety margin). Seven planes, 5 mm apart from each other, were therefore identified, from the phantom surface to the maximum depth of cut. Seven trajectories were thus designed, 2 mm of thickness each. The trajectories are initially all disabled; the system detects the position of the scalpel tip and automatically switches on the correct trajectory depending on the depth reached by the scalpel along the insertion axis. Figure 4 illustrates two snapshots of what the user was seeing projected onto the displays during the execution of the task. The users were asked to cut along all the trajectories in order to create the enucleation cylinder, which could then be extracted and examined.

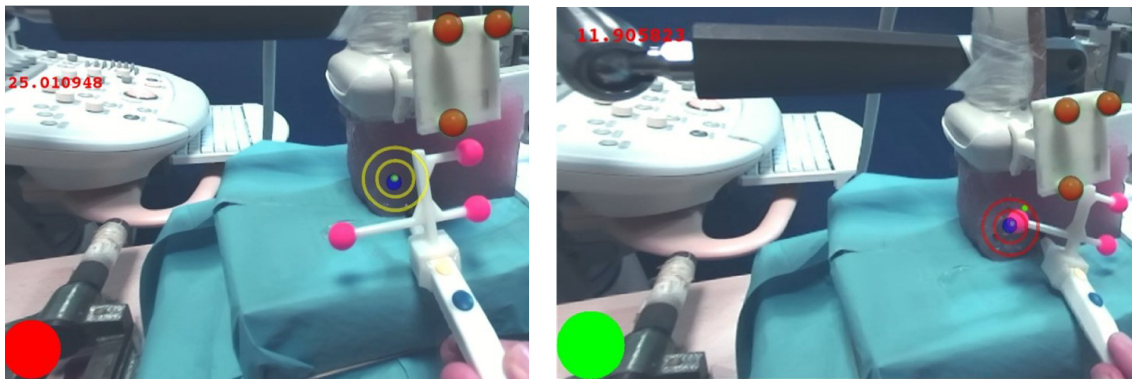


**FIGURE 4** Snapshots of a single display during the execution of the task. On the left: in the earliest stages of the procedure, a trajectory near the surface is illuminated (recognisable by its yellow colour). Note the red semaphore indicating that the scalpel tip is within the inner circumference (green sphere clearly visible above the blue virtual lesion). On the right: further in the procedure, a deeper trajectory is switched on (red trajectory). The green semaphore indicates the correctness of the scalpel tip position, clearly visible within the virtual track.

## 4.3 | Results and discussion

At the end of each procedure, the enucleated portion was rescanned with the US probe to check that the lesion had been removed without damage and that the safety margins had been respected. From a qualitative analysis of the enucleations, it was observed that all users were able to remove the lesion without ever incising it, an essential requirement in the excision of a tumour as the spread of the malignant tissue must be avoided. However, not all the users were able to meet the safety margin of 1 cm around

the lesion. Figure 5 shows the worst case with an indication of the margins. The results are nevertheless promising if we consider that none of the users who performed the enucleations was a clinician.

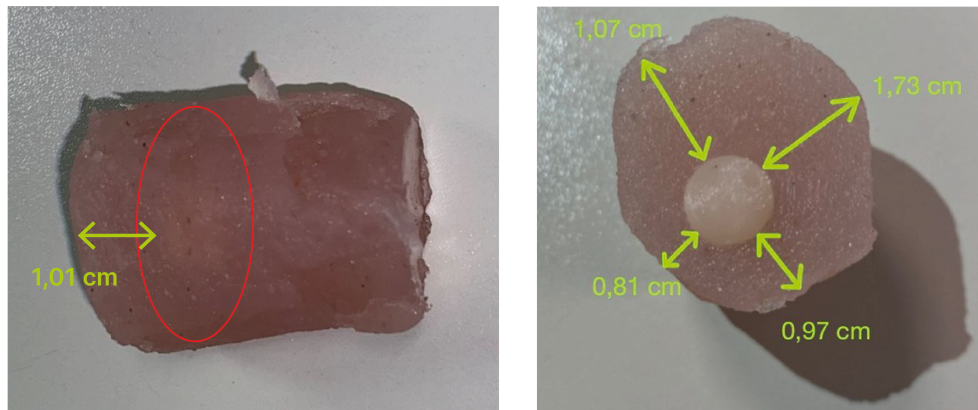


**FIGURE 5** Enucleation cylinder excised by one of the four users. Outlined in yellow are the safety margins left around the lesion.

This user study on phantoms was intended to evaluate the usability, feasibility, and reliability of the AR guidance. Given the preliminary nature of the user study (four non-expert users on non-anthropomorphic phantoms), the assessment made is purely qualitative (i.e., checking that the lesion was within the enucleation cylinder and that safety margins were met). However, the choice to test the system only with non-expert users was intentional. We assumed indeed that non-clinical users would be unencumbered by pre-existing knowledge of the enucleation task and would thus have to rely totally on the AR guidance provided through the HMD. In this way, we could be sure that a positive test result (i.e., complete enucleation of the lesion with preservation of the proper safety margins), was due to the accuracy of the virtual guidance provided to the user and not to his or her prior skills.

The positive results of this preliminary test lead to the design of a more comprehensive and structured user study, ideally on anthropomorphic phantoms, which will include both experienced and inexperienced users, in order to perform both intra- and inter-operator comparative evaluations.

## 5 | CONCLUSION

Pursuing a line of research increasingly addressed in recent literature, namely the employment of wearable AR systems for the in-situ visualization of US images to guide interventions, in this work we propose the first AR system for guiding in-depth tumour enucleation procedures. We devised an innovative visualization modality that allows the operator to have the correct guidance at all depths and regardless of the point of view. In our system, in fact, the tracking of the surgical tool allows the cutting trajectory to be automatically adapted according to the depth reached by the instrument. In addition, the implementation of a virtual-to-virtual alignment, combined with the chromatic information provided through the semaphore, allows the operator to never lose sight of the instrument tip, even when it is deep in the tissue. Accuracy tests showed that the system can provide the position of the scalpel tip with high accuracy both in terms of depth to the target (mean depth error 0.4 mm) and radially to an ideal insertion axis (mean radial error 1.34 mm). The preliminary study carried out with four non-expert users indicated that the AR system and the visualization modality proposed can be used to successfully guide the enucleation of in-depth lesions: all users were able to excise the lesion without damaging it and, for the most part, also meeting the safety margins required by the procedure.

### AUTHOR CONTRIBUTIONS

Conceptualization, N.C., F.C. and V.F.; methodology, N.C. and L.L.; software, F.C. and N.C.; validation, L.L., N.C. and F.C.; formal analysis, N.C. and F.C.; investigation, N.C.; resources, V.F.; data curation, N.C. and L.L.; writing—original draft preparation, N.C.; writing—review and editing, N.C.; visualization, N.C. and V.F.; supervision, V.F.; project administration, V.F.; funding acquisition, V.F. All authors have read and agreed to the published version of the manuscript.

## ACKNOWLEDGMENTS

We acknowledge the support of the European Union by the Next Generation EU project ECS0000017 'Ecosistema dell'Innovazione' Tuscany Health Ecosystem (THE, PNRR, Spoke 9: Robotics and Automation for Health), and the Italian Ministry of Education and Research (MUR) in the framework of the FoReLab and CrossLab projects (Departments of Excellence).

## CONFLICT OF INTEREST

The authors declare no potential conflict of interest.

## REFERENCES

1. Zhao Z, Poyhonen J, Cai XC, et al. Augmented reality technology in image-guided therapy: State-of-the-art review. *Proceedings of the Institution of Mechanical Engineers, Part H: Journal of Engineering in Medicine*. 2021;235(12):1386-1398. PMID: 34304631doi: 10.1177/09544119211034357
2. Sielhorst T, Feuerstein M, Navab N. Advanced Medical Displays: A Literature Review of Augmented Reality. *Journal of Display Technology*. 2008;4(4):451-467. doi: 10.1109/JDT.2008.2001575
3. Kersten-Oertel M, Jannin P, Collins DL. The state of the art of visualization in mixed reality image guided surgery. *Computerized Medical Imaging and Graphics*. 2013;37(2):98-112. doi: 10.1016/j.compmedimag.2013.01.009
4. Fuchs H, State A, Pisano ED, et al. Towards performing ultrasound-guided needle biopsies from within a head-mounted display. In: Höhne KH, Kikinis R., eds. *Visualization in Biomedical Computing* Springer Berlin Heidelberg 1996; Berlin, Heidelberg:591–600.
5. Rosenthal M, State A, Lee J, et al. Augmented reality guidance for needle biopsies: An initial randomized, controlled trial in phantoms††A preliminary version of this paper was presented at the Medical Image Computing and Computer-Assisted Intervention (MICCAI) 2001 conference in Utrecht, The Netherlands (Rosenthal et al., 2001). *Medical Image Analysis*. 2002;6(3):313-320. Special Issue on Medical Image Computing and Computer-Assisted Intervention - MICCAI 2001doi: [https://doi.org/10.1016/S1361-8415\(02\)00088-9](https://doi.org/10.1016/S1361-8415(02)00088-9)
6. Sauer F, Khamene A, Bascl B, Schinunang L, Wenzel F, Vogt S. Augmented reality visualization of ultrasound images: system description, calibration, and features. In: 2001:30-39
7. Kanithi PK, Chatterjee J, Sheet D. Immersive Augmented Reality System for Assisting Needle Positioning during Ultrasound Guided Intervention. In: ICVGIP '16. Association for Computing Machinery 2016; New York, NY, USA
8. Rüger C, Feufel MA, Moosburner S, Özbek C, Pratschke J, M. SI. Ultrasound in augmented reality: a mixed-methods evaluation of head-mounted displays in image-guided interventions. *International Journal of Computer Assisted Radiology and Surgery*. 2020;15(11):1895-1905. doi: 10.1007/s11548-020-02236-6
9. Farshad-Amacker NA, Bay T, Roskopf AB, et al. Ultrasound-guided interventions with augmented reality in situ visualisation: a proof-of-mechanism phantom study. *European Radiology Experimental*. 2020;4(1). doi: 10.1186/s41747-019-0129-y
10. Cattari N, Condino S, Cutolo F, Ferrari M, Ferrari V. In Situ Visualization for 3D Ultrasound-Guided Interventions with Augmented Reality Headset. *Bioengineering*. 2021;8(10). doi: 10.3390/bioengineering8100131
11. Haxthausen vF, Rüger C, Sieren MM, Kloeckner R, Ernst F. Augmenting Image-Guided Procedures through In Situ Visualization of 3D Ultrasound via a Head-Mounted Display. *Sensors*. 2023;23(4). doi: 10.3390/s23042168
12. Xu C, Lin C, Xu Z, Feng S, Zheng Y. Tumor Enucleation vs. Partial Nephrectomy for T1 Renal Cell Carcinoma: A Systematic Review and Meta-Analysis. *Frontiers in Oncology*. 2019;9. doi: 10.3389/fonc.2019.00473
13. Cattari N, Condino S, Cutolo F, Ghilli M, Ferrari M, Ferrari V. Wearable AR and 3D Ultrasound: Towards a Novel Way to Guide Surgical Dissections. *IEEE Access*. 2021;9:156746-156757. doi: 10.1109/ACCESS.2021.3129324
14. Ferrari V, Cutolo F. Letter to the Editor: Augmented reality-guided neurosurgery. *Journal of Neurosurgery JNS*. 2016;125. doi: 10.3171/2016.1.jns153040
15. Trivisio, Lux Prototyping. .
16. Cutolo F, Cattari N, Carbone M, D'Amato R, Ferrari V. Device-Agnostic Augmented Reality Rendering Pipeline for AR in Medicine. In: 2021:340-345
17. Intoy J, Rucci M. Finely tuned eye movements enhance visual acuity. *Nature Communications*. 2020;11(1). doi: 10.1038/s41467-020-14616-2
18. Cutolo F, Freschi C, Mascioli S, Pardi PD, Ferrari M, Ferrari V. Robust and Accurate Algorithm for Wearable Stereoscopic Augmented Reality with Three Indistinguishable Markers. *Electronics*. 2016;5(3). doi: 10.3390/electronics5030059
19. Mahmoud MZ, Aslam M, Alsaadi M, Fagiri MA, Alonazi B. Evolution of Robot-assisted ultrasound-guided breast biopsy systems. *Journal of Radiation Research and Applied Sciences*. 2018;11(1):89-97. doi: <https://doi.org/10.1016/j.jrras.2017.11.005>
20. Welleweerd FJ, Groenhuis V, Veltman J, Stramigioli S. Design of an end-effector for robot-assisted ultrasound-guided breast biopsies. *International Journal of Computer Assisted Radiology and Surgery*. 2020;15(4):681-690. doi: 10.1007/s11548-020-02122-1
21. Do TD, LaViola JJ, McMahan RP. The Effects of Object Shape, Fidelity, Color, and Luminance on Depth Perception in Handheld Mobile Augmented Reality. In: 2020:64-72